Classification
Physics Abstracts
81.40.Np — 07.05.Pj — 81.70.Yp

Roughness and $\mathbb{R}^2 \times \mathbb{R}$ Function Analysis: Applications in Material Science

Michel Coster, Gervais Gauthier, Séverine Mathis and Jean-Louis Chermant

LERMAT, URA CNRS 1317, ISMRA, 6 bd Maréchal Juin, 14050 Caen Cedex, France

Résumé. — La rugosité des surfaces non planes sans parties cachées peut être étudiée à partir de l'analyse des fonctions de type $\mathbb{R}^2 \times \mathbb{R}$. Ces fonctions correspondent soit à la vraie topographie soit à une vue en perspective. Elles peuvent être décrites quantitativement à partir des paramètres stéréologiques de base sur l'image elle même ou après transformations morphologiques. Quelques exemples sont donnés en sciences des matériaux en utilisant un MEB ou un microscope confocal.

Abstract. — In the case of absence of overlaps, roughness investigation can be studied from $\mathbb{R}^2 \times \mathbb{R}$ function analysis methods. These $\mathbb{R}^2 \times \mathbb{R}$ functions correspond to a true topography or a perspective representation. They can be quantitatively described directly from basic stereological parameters or after morphological transformations. Some examples in material science are given using scanning electron or confocal microscope images.

Introduction

In material science, two ways of morphological analysis are used. The first one allows to characterize the morphology of bulk material by means of metallographic plane sections. The second one is less often used: it allows to characterize the external surface of a material. This kind of analysis is important in many fields such as fractography, roughness studies on metallic sheets or skin, corrosion, and so on. In this paper, first different image acquisitions will be briefly commented. Secondly, the main parameters and morphological functions with their properties will be presented. Finally some examples with images obtained by scanning electron microscope (SEM) or confocal microscopes will be given.

Scanning Electron Microscope and Confocal Microscope Images

From non planar surfaces without overlaps, the corresponding grey tone images can be obtained by two ways. With a confocal microscope or a 3D roughness instrument, the grey tone image gives the *true relief*. The radiometric value of each pixel is proportional to the altitude of each point. The proportionality coefficient is computed from the calibration.

The SEM gives a *perspective image* where the value of each pixel does not correspond to the altitude. With this instrument, a modification of contrast and brightness adjustments changes the grey values of the image: an *anamorphosed* (a monotonous increasing change of the grey scale) image of the previous one is obtained without a possibility of calibration. When overlaps exist, the non planar surface must be cut by an approximately perpendicular plane. So a profile is obtained which can be observed with SEM or optical microscope and can be analysed [1, 2]. The profilometric analysis gives metric information on roughness), but it is impossible to know the surface roughness without modelling and connectivity measurements are not accessible.

Basic Parameters

In the case of absence of overlaps, the basic parameters for $\mathbb{R}^2 \times \mathbb{R}$ functions [3, 4] can be used. According to the set meaning, a $\mathbb{R}^2 \times \mathbb{R}$ function f is characterized by its *support* Z and its area $A(Z)$, by the surface $S(G(f))$ of its *graph* $G(f)$, and by the volume $V(\mathrm{SG}(f))$ of its *subgraph* $\mathrm{SG}(f)$. The third metric property of the function is given by the integral of *connectivity*, $N_2(f)$, which corresponds to the sum of the local maxima heights minus the sum of local minima heights. In the local case, these parameters can be estimated by unit area of the support. So, one obtains: the volume per unit area of support $V_A(f)$, the surface area per unit area of support $S_A(f)$ and the integral of connectivity number per unit area of support $N_A(f)$.

To these three metric parameters, one can add two topological ones: the *number of local maxima heights*, $(N_2(\max(f)))$, and the *number of local minima heights*, $(N_2(\min(f)))$. These two last parameters are very sensitive to the noise. They can be replaced respectively by the *number of local maxima having a "local" height greater than h, (max of size h, $N_2(h\max(f))$)*, and by *the number of local minima having a "local" depth greater than h, (min of size h, $N_2(h\min(f))$)*, [5].

In the local case, the parameters for the max become the number of max or max of size h per unit area of support $N_A(\max(f))$ $N_A(h\max(f))$. For the min in the local case, these parameters become the number of min or min of size h per unit area of support $N_A(\min(f))$ $N_A(h\min(f))$. The functions $\min(f)$, and $h\min(f)$ are obtained from *geodesic reconstruction of the function* $(f + \delta)$ or $(f + h)$ *over the function* f. They are noted respectively $R^f(f + \delta)$ and $R^f(f + h)$. The function $\max(f)$ and $h\max(f)$ are also obtained from *geodesic reconstruction of the function* $(f - \delta)$ or $(f - h)$ *under the function* f. They are noted respectively $R_f(f - h)$ and $R_f(f - \delta)$. δ represents the smallest interval h in grey level range. The functions $f - R_f(f - h)$ and $R^f(f + h) - f$ are called respectively h *convex* and h *concave function*. $V_A(f)$ corresponds to the mean value of the function (mean altitude). Thus this parameters is not interesting for itself, but very useful for granulometry and roughness functions (see later). $S_A(f)$ is equivalent to the *surface roughness* and $N_A(f)$ equivalent to the *vertical roughness for surface*. In the case of perspective images, these two last parameters depend on anamorphosis [6]. The number of max or min for $h = \delta$ does not depend on anamorphosis, but they are not robust parameters. As opposed, for the max and min of size h, the parameters are less sensitive to the noise, but vary with anamorphosis. These last parameters could be applied on SEM images of ceramic powders to separate two kinds of powder [7-9].

Morphological Functions

ANAMORPHOSIS PROBLEM AND SOLUTION. — Morphological functions are built from transformations which are applied to functions. Two kinds of structuring element can be used, *volumic* and *flat structuring element*. In the case of flat elements, where morphological transformation is used, the "absolute result" is always different from the result obtained for volumic elements.

But the "relative result" is the same when a flat structuring element is used. So, the ratio between basic measurements performed on the transformed image and on the initial (reference) image is always the same and is independent on the anamorphosis.

GRANULOMETRIC FUNCTIONS. — The granulometry [10, 11] is the first morphological function used to describe non planar surfaces represented by $\mathbb{R}^2 \times \mathbb{R}$ functions [12, 13]. A granulometry is obtained from opening or closing transformation with *a convex structuring element* λB, which depends on size parameter λ. The granulometric distributions are given by:

$$G(f_{\lambda B}) = \frac{V(f) - V(O^{\lambda B}(f))}{V(f)} \quad \text{and} \quad G(f_{\lambda B}) = \frac{V(F^{\lambda B}(f)) - V(f)}{V(f)}$$

where $O^{\lambda B}(f)$ is the opening transformation and $F^{\lambda B}(f)$ the closing one. When the structuring element λB is flat, the granulometric distribution is independent on anamorphosis. This tool allows to quantitatively characterize the morphological evolution according to the chosen manufacturing process [13].

SURFACE ROUGHNESS FUNCTION. — By definition [14, 15], the *roughness function* is defined by the evolution of the surface area of the graph as a function of the size of the gauge used to perform measurements. In the local case, the surface area is replaced by $S_A(f)$. This parameter was used with success on true relief of corroded aluminium observed by confocal microscopy to follow the evolution of roughness during etching [8, 16]. To estimate $S_A(f)$, Steiner's method (difference between dilated and eroded sets) is used. Thus the absolute surface roughness function is given by:

$$S_A(f, \lambda) = \frac{S(f, \lambda)}{A(Z)} = \frac{V(D^{\lambda B}(f)) - V(E^{\lambda B}(f))}{2\lambda \times A(Z)}.$$

It should be noted that $S(f, \lambda)$ is equivalent to the modulus of morphological gradient [17] measured at different scales λ. In these conditions $S_A(f, \lambda)$ depends on anamorphosis for all classes of structuring elements. This is the reason why we have proposed another function *called relative surface roughness function* defined by equation:

$$R_S(f, \lambda) = \frac{S_A(f, \lambda)}{S_A(f, \lambda_0)}$$

where λ_0 is the smallest size of structuring element. The result is independent on the anamorphosis when structuring element is flat. This parameter can be used to draw a fractal plot, but carefully. Indeed the right value of the fractal dimension is obtained with a flat structuring element. But when $\lambda \to \infty$, the slope reaches asymptotically the value 1. This is not the case with a volumic structuring element. The roughness function was used to characterize some fracture surfaces as brittle fracture of alumina or ductile fracture of steel [14], (Figs. 1 and 2). These analysis are compared with an analysis performed on simulated surfaces (Boolean and fractal surfaces) (Figs. 3 and 4). The roughness functions of fracture surface are closer to the fractal model than to the Boolean one. A fractal analysis proves that these surfaces can be described exactly by a fractal model.

Flood Transformations

To describe quantitatively this topology or topography on $\mathbb{R}^2 \times \mathbb{R}$ functions, one must use another kind of morphological process, the *flood transformations*. It is possible to define several

Table I. — *Definitions of flood transformations.*

Flood model	Flood function	Filling function
Immersion	$\mathrm{imm}(f, h) = \mathrm{Sup}(f, h \min(f))$	$R_{\mathrm{imm}}(f, h) = \mathrm{imm}(f, h) - f$
Lower inundation	$L \, \mathrm{inund}(f, h) = h \min(f)$	$R_{\mathrm{inund}}(f, h) = h \, \mathrm{concave} \, (f)$
		$R_{\mathrm{inund}}(f, h) = h \min(f) - f$
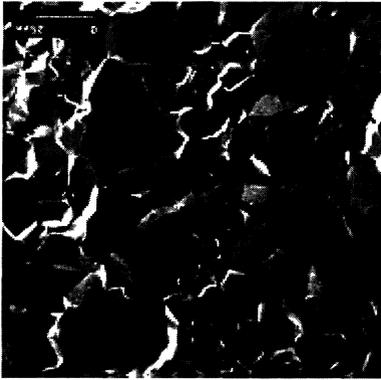
Fig. 1.

Fig. 2.

Fig. 1. — Brittle fracture of alumina.
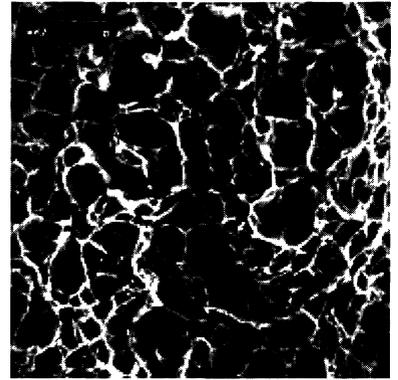
Fig. 2. — Ductile fracture of steel.
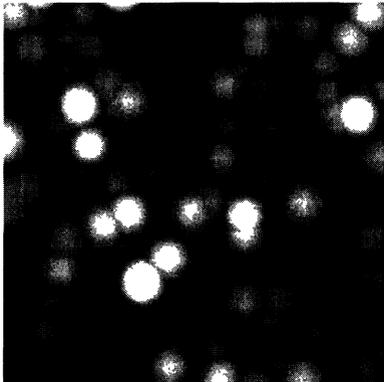
Fig. 3.

Fig. 4.

Fig. 3. — Simulation of a boolean surface.
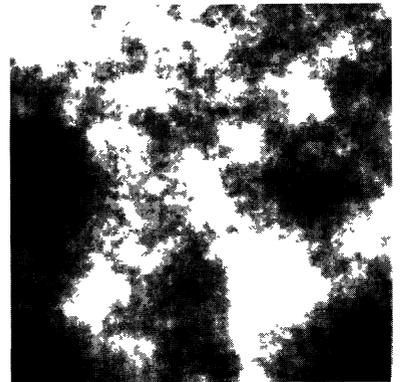
Fig. 4. — Simulation of a fractal surface.

Fig. 5.   Fig. 6.
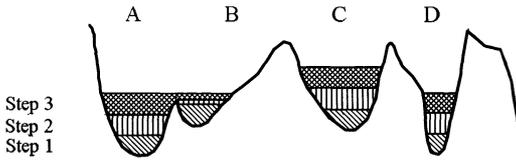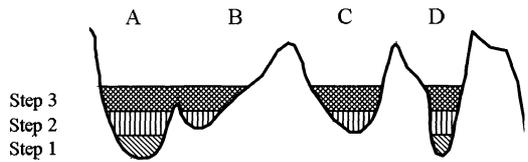
Fig. 5. — Lower inundation.
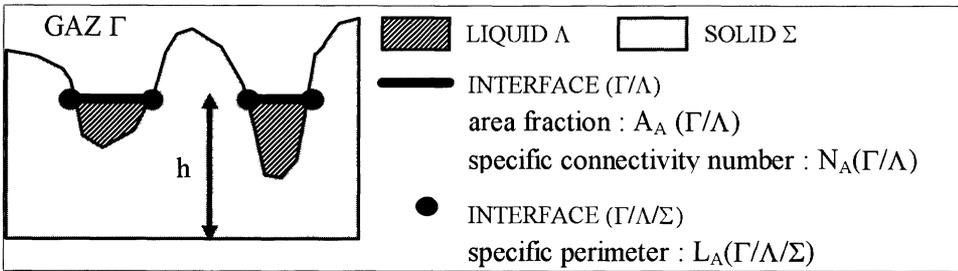
Fig. 6. — Immersion.

Fig. 7. — Flood parameters and their signification.

flood transformations, slightly different from physical flood. Gauthier [15] proposed two models: *lower inundation* (Fig. 5) *and immersion* (Fig. 6). Table I gives the equivalent morphological transformations. The corresponding *filling functions* are also defined.

Measures on Flood Transformations

Since each flood transformation gives another $\mathbb{R}^2 \times \mathbb{R}$ function, it is possible to perform the classical measurements on the resulting image and to follow the value of these parameters as a function of h. Before flood processes, the $\mathbb{R}^2 \times \mathbb{R}$ functions can be considered as a two phases system, the subgraph called "solid phase Σ" and the upper graph called "gas phase Γ". After flood transformation appears a new phase, "the liquid phase Λ". Thus it is possible to follow the parameter related to each phase or interface between phases. Figure 7 gives these different parameters in terms of phase or interphase.

Evolution of Parameters as a Function of Flood Parameter h

To understand the use of these parameters, one gives some examples of evolution in the case of the immersion process which is the simplest method. In many cases $A_A(\Gamma/\Lambda) = f(h)$ changes according to sigmoïdal curves between 0 to 1, and the curve is more and less symmetric (Fig. 8). It corresponds directly to a flood process. $N_A(\Gamma/\Lambda) = f(h)$ has a more complex shape which can be explained easily, (Fig. 9). To understand this evolution, one must imagine that the relief is progressively immersed in the sea. For each step of immersion, the connectivity number gives the number of lakes or closed seas. The evolution of the specific perimeter $L_A(\Gamma/\Lambda/\Sigma) = f(h)$ is illustrated in figure 10. The increasing part of the curve corresponds to lake formation and
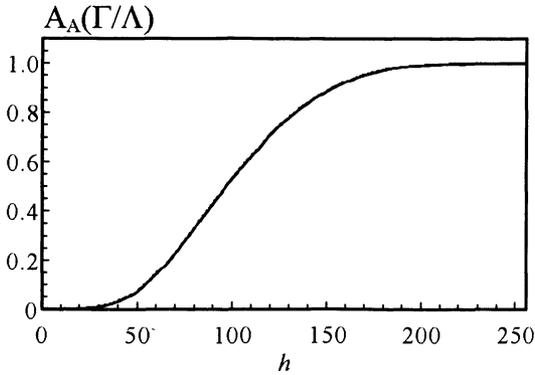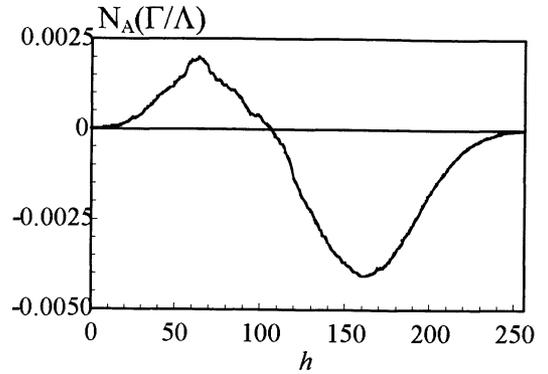
$A_A(\Gamma/\Lambda)$

Fig. 8.

$N_A(\Gamma/\Lambda)$

Fig. 9.

Fig. 8. — Area fraction of the liquid-gas interface (Γ/Λ) according to the level h of immersion (fracture surface of steel).

Fig. 9. — Specific connectivity number of the liquid-gas interface (Γ/Λ) according to the level h of immersion.
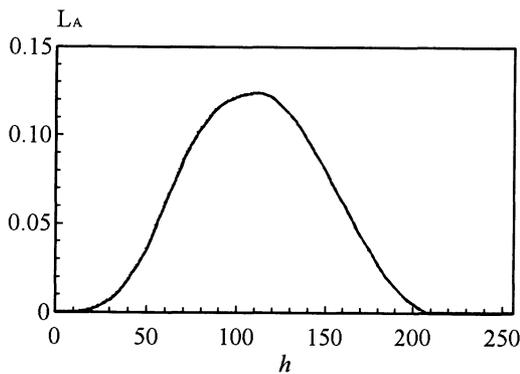
L_A

Fig. 10. — Evolution of the specific parameter $L_A(\Gamma/\Lambda/\Sigma)$ according to the level h of immersion (fracture surface of steel).

growing. But after a certain time some connection appears and the specific perimeter decreases towards zero. The maximum value of the function corresponds to the zero value of $N_A(\Gamma/\Lambda)$. The more and less symmetric shapes of the curves give information on the symmetry of relief.

Conclusion

Several morphological tools to describe quantitatively the non planar surfaces were presented in this paper. The basic parameters derived from the stereology are classical. To obtain more information, functions derived from mathematical morphology are also presented. The first ones (granulometric and roughness functions) are relatively classical. The inundation functions give information on the topology of the surface.

Acknowledgements

References

[1] El Soudani S.M., *Metallography* **11** (1978) 245.

[2] Chermant J.L. and Coster M., Mathematical morphology and quantitative fractography. 7th International Congress of Fracture, Houston, Tx, 19-24 March 89, K. Salama, K. Ravi-Chandar, D.M.R. Taplin, P. Rama-Rao Eds. (1989) p. 3373.

[3] Coster M., *Acta Stereol.* **11** (1992) 639.

[4] Hénault E. and Chermant J.L., *Acta Stereol.* **11** (1992) 665.

[5] Grimaud M., La géodésie numérique en morphologie mathématique. Application à la détection automatique de microcalcifications en mammographie numérique. Thèse de Doctorat de l'École Nationale Supérieure des Mines de Paris (1991).

[6] Hénault E., Caractérisation géométrique d'images en niveaux de gris : application à l'analyse des surfaces non planes, Thèse de Doctorat de l'Université de Caen (1992).

[7] Mathis S. and Coster M., *Acta Stereol.* **14** (1995) 201.

[8] Mathis S., Acquisition et analyse quantitative des images de microreliefs en microscopie confocale et en microscopie électronique à balayage. Thèse de Doctorat de l'Université de Caen (1996).

[9] Coster M., Prod'homme M., Chermant L. and Chermant J.L., *Microsc. Microanal. Microstructr.* **7** (1996) 407.

[10] Matheron G., Random Sets and Integral Geometry (Wiley, New York, 1975).

[11] Serra J., Image Analysis and Mathematical Morphology (Academic Press, London, 1982).

[12] Michelland S., Schiborr B., Coster M., Mordike B.L. and Chermant J.L., *J. Microsc.* **156** (1989) 303.

[13] Prod'homme M., Chermant L. and Coster M., *Acta Stereol.* **11** (1992) 261.

[14] Coster M., Gauthier G. and Chermant J.L., Roughness investigation by mathematical morphology. STERMAT'94, Proceedings edited by L. Wojnar (Fotobit Design, Beskidy Mountains Poland, 1994) p. 201.

[15] Gauthier G., Applications de la morphologie mathématique fonctionnelle: analyse des textures en niveaux de gris et segmentation par approche multimodale, Thèse de Doctorat de l'Université de Caen (1995).

[16] Mathis S. and Coster M., *Microsc. Microanal. Microstructr.* **7** (1996) this issue.

[17] Beucher S., Morphologie mathématique et segmentation, Thèse de Docteur-Ingénieur de l'École des Mines de Paris (1990).